Mon. Not. R. Astron. Soc. **000**, 1–15 (2011) Printed 18 May 2011 (MN LATEX style file v2.2)

Young clusters and massive black holes as the building blocks of ultra-compact dwarf galaxies

Pau Amaro-Seoane[1,2] ⋆, Symeon Konstantinidis[1,3], Marc Dewi Freitag[4,5], M. Coleman Miller[6] & Frederic M. Rasio[7]

[1] *Max Planck Institut für Gravitationsphysik (Albert-Einstein-Institut), D-14476 Potsdam, Germany*
[2] *Institut de Ciències de l'Espai (CSIC-IEEC), Campus UAB, Torre C-5, parells, 2na planta, ES-08193, Bellaterra, Barcelona, Spain*
[3] *Department of Physics, Aristotle University of Thessaloniki, Thessaloniki 54124, Greece*
[4] *Institute of Astronomy, Madingley Road, CB3 0HA Cambridge, UK*
[5] *Gymnase de Nyon, Route de Divonne 8, 1260 Nyon, Switzerland*
[6] *Department of Astronomy and Maryland Astronomy Center for Theory and Computation, University of Maryland, College Park, MD 20742-2421, USA*
[7] *Department of Physics and Astronomy, Northwestern University, Evanston, IL 60208, USA*

draft 18 May 2011

ABSTRACT

The origin and evolution of ultra-compact dwarf galaxies is a conundrum. Why do we care about the problem. **GAIA?** The relevance of the massive black hole at the centre of the system is... HST observations reveal regions of a few hundreds of pc in nteracting galaxies such as the Antennæ that harbour amalgamations of young clusters. This is probably due to the fact that two colliding galaxies trigger intense bursts of stellar formation. Such young stellar clusters are deemed to be the formation place of black holes with masses ranging between 10^2 and $10^4\,M_\odot$. A fraction of the clusters is bound and the cluster binary doomed to merge. The central BHs form a binary which coalesce in about ~ 7 Myrs after an intense burst of gravitational radiation, measurable with ground-based interferometers like LIGO and VIRGO. The gravitational radiation recoil can generate strong enough kicks to eject the resulting single black hole from the merged cluster. In this work we address the joint evolution of such a cluster complex (CC) and the interaction with a recoiling massive black hole, as well as the implications on the formation of a seed ultra-compact dwarf galaxy (UCD). For this, we run a set of detailed simulations for individual interaction of the recoiling MBH and the young clusters and follow the dynamical evolution of the CC and the process of agglomeration of clusters in its centre. In our fiducial model we find that the recoiling MBH is captured in the forming UCD after hitting many clusters. In the process it triggers stellar disruptions and, thus, flares of electro-magnetic radiation. The hole is retained in the most likely cases of realistic initial mass functions for the CC. Later and in a time shorter than typically a few hundred Myrs, the MBH sinks down to the very centre of the UCD seed. Depending on the ocupation fraction of MBHs in such clusters, the sinking holes can contribute significantly to the future central massive black hole of the formed UCD. Since they sink rather quickly as compared to the formation process of the UCD, we expect that UCD can be a prominent source of gravitational radiation and that the central black hole could be orders of magnitude larger than one expects from standard formation scenarios of UCD. **Implications for cosmology, if any?**

Key words: galaxies: dwarf – galaxies: interactions – galaxies: kinematics and dynamics – galaxies: star clusters: general – gravitational waves – methods: numerical

1 INTRODUCTION

Bound systems of young, massive clusters are found in many observations of colliding galaxies. The most stud-

⋆ E-mail: Pau.Amaro-Seoane@aei.mpg.de (PAS, corresponding author)

ied case is the Antennæ galaxies (NGC 4038/4039) which is the nearest example of colliding disk galaxies that are listed in the Toomre (1977) sequence. In this young merging galaxy, Hubble Space Telescope observations revealed the existence of many relatively small areas harboring hundreds of young clusters (Whitmore et al. 2010, 1999; Whitmore 2006). Whitmore et al. (2010) observed 18 areas ("knots") with sizes of 100−600pc containing hundreds of clusters. The mass function of those systems, which we will call henceforth Cluster Complexes (CCs) has been studied in detail by Zhang & Fall (1999) who concluded that the observed clusters, with masses $10^4 - 10^6 M_\odot$ follow a power law distribution with index n $= -2$. Bastian et al. (2006) found that in the Antenæ galaxy there are also low-mass CCs with masses around $10^6 \mathrm{M}_\odot$ and diameters $100 - 200$pc. Some of their observed CCs have radii greater than their tidal radii which means that those CCs will lose some of their clusters or individual stars, which will be still trapped by the gravitational field of the galaxy. One of the most studied CCs is the "knot S" with a total mass of $10^8 \mathrm{M}_\odot$ and a total radius of ~ 450pc (Whitmore et al. 1999). The number of observed clusters in this CC is of around 100 with the most massive one having a mass of about $1.63 \times 10^6 \mathrm{M}_\odot$ (Whitmore et al. 2010). The number of CCs found in other merging galaxies is continuously increasing mainly because of the improvements in the observational instruments and techniques. CCs have been found in NGC7673 (Homeier et al. 2002), in M82 (Konstantopoulos et al. 2009), in NGC6745 (de Grijs et al. 2003), in the Stephan's Quintet (Gallagher et al. 2001) and in NGC 922 (Pellerin et al. 2010).

CCs are bound systems (Kroupa 1998; Fellhauer & Kroupa 2005; Bruens et al. 2011; Whitmore et al. 2010) and in relatively short time-scales at least some of their member-clusters will merge to form a single object. Kroupa (1998); Fellhauer & Kroupa (2005) used $N-$body simulations to show that CCs might be the progenitors of Ultra-Compact Dwarf Galaxies (UCDs). Recently Bruens et al. (2011) performed $N-$body simulations of CCs covering a large fraction of the parameter space using different total masses ($10^{5.5} - 10^8 \mathrm{M}_\odot$) and initial Plummer radii $10-160$pc. Their conclusions indicate that objects such as UCDs, Extended Clusters (ECs) or even large Globular Clusters (GCs) that are observed in today's galaxies, might have formed by merging CCs. According to their simulations, almost all cluster-members of a CC would merge in less than 1Gyr, while in some cases the merging time would be of the order of 10Myr. The final product could contain $26 - 97\%$ of the mass of the initial CC and could be as large as 55pc.

The repeated mergers of clusters in CCs might be interesting not only for the formation of large GCs or a UCDs, but also for gravitational radiation astronomy. Theoretical and numerical studies show that at least a fraction of young star clusters could host intermediate-mass Black Holes (MBHs, black holes with masses ranging between $10^{2-4}\, M_\odot$) at their centres. In a young cluster, the most massive stars sink down to the centre due to mass segregation. After a high-density stellar region forms, stars start to collide and merge with eachother. A number of numerical studies with rather different approaches, show that, under these circumstances, one of the stars increases its mass exponentially in a process denominated "runaway growth" (Portegies Zwart & McMillan 2000; Gürkan et al. 2004; Portegies Zwart et al. 2004; Freitag et al. 2006a,b). Freitag et al. (2006b,a) found the precise requirements to form a massive black hole (MBH) in the centre of the host cluster. If there are not "too hard" binaries, the time to reach core-collapse is shorter than 3 Myr and the velocity dispersion is not much larger than $\sim 500\,\mathrm{yr}^{-1}$, the mass of the VMS formed is $\gg 100\, M_\odot$. The later evolution of this star is not well understood, nor are the necessary conditions that it not evolve into a super-massive star (see Amaro-Seoane & Spurzem 2001; Amaro-Seoane et al. 2002; Amaro-Seoane 2004, and the references in their work), nor the limits on the mass not to collapse into an MBH. The process depends on the metallicity, winds (see e.g. Belkus et al. 2007, though it is not well defined how to extrapolate the results, limited to stars with masses of maximum $150\, M_\odot$ to the masses of relevance, of at least one order of magnitude larger) and the collisions on to the runaway star. We note that Suzuki et al. (2007) investigated the growth of a runaway process by compounding direct $N-$body simulations with smooth particle hydrodynamics (SPH). They found that stellar winds would not cramp the formation of the VMS.

Although their existence has not been verified by observations, the list of clusters that might contain an MBH is growing (van der Marel & Anderson 2010; Noyola et al. 2010; Gebhardt et al. 2005; Ptak & Colbert 2004; Colbert & Miller 2005). For this work, we will accept their existence as a working assumption or ansatz.

Amaro-Seoane & Freitag (2006) showed that mergers of two clusters containing MBHs at their centres would lead to the formation of an MBH binary, which would merge in a time scale as short as $\sim$ 7Myr. Such merger could be easily detected with ground-based detectors such as Advanced LIGO or Advanced VIRGO if the event happens within the observable volume of the detector (Amaro-Seoane & Santamaria 2009). Numerical relativity simulations show that during the merger of two black holes, gravitational radiation is emitted asymmetrically with the size of asymmetry depending on the mass ratio of the two black holes and on their spin magnitude and orientation (see e.g. Rezzolla 2009,for a review). If this recoiling velocity exceeds the average velocity dispersion of the merged cluster, then the MBH leaves it and makes its way out to the CC. This asymmetry in the emission of gravitational radiation leads to a recoil velocity of the resulting system (Zlochower et al. 2010; Gonzalez et al. 2007; Lousto & Zlochower 2008; Baker et al. 2008; Lousto et al. 2010a; Campanelli et al. 2007a,b; Healy et al. 2009; Pretorius 2005; Sopuerta et al. 2006). Depending on the mass ratio, the spins and the spin orientation with respect to the plane of the inspiral orbit of the two black holes the magnitude of the recoil velocity might be as high as $4000\mathrm{km\,s}^{-1}$ (Lousto & Zlochower 2010), with the expected values being at least one order of magnitude lower. Statistical studies of the recoil velocities for different mass-ratios and spins show that the expected recoil velocities are between $100 - 300\mathrm{km\,s}^{-1}$ (Lousto et al. 2010b).

In this article we present results that address the question of formation of ultra-compact dwarf galaxies by the agglomeration of young clusters in CC and the role of a recoling MBH which we assume to have formed by the merger of two clusters. In section 2 we give an estimate on the recoiling velocity that the MBH will have after formation. Depending on the magnitude of it, the MBH will interact with other

clusters in the CC or not. In section 3 we analyse the interaction of a MBH recoiling through the CC and the individual clusters. For this, we have made a comprehensive numerical study of ~ 200 direct-summation $N-$body simulations that covers the parameter space in detail, in particular the mass ratios, relative velocity and impact parameter. Later, in section 4 we describe the larger-scale simulations and the main results, i.e. how we follow the dynamical evolution of the CC and the amalgamation of clusters, which will lead to a "seed" UCD. Of particular interest for us is the interplay between the MBH and the individual clusters. For this we use the grid of simulations presented in the previous section, which help us to correct for the orbital parameters of the MBH. Finally, in section 5 we present our main conclusions of the work.

2 INITIAL RECOILING VELOCITY OF THE MBH

In this section we calculate the most likely recoiling velocity the final MBH will have in a scenario as described in Amaro-Seoane & Freitag (2006). The authors study the merger of two clusters harbouring each one a MBH. They find that after some 7 Myrs the binary will coalesce due to the emission of gravitational radiation. For that aim, we run a set of experiments in order to study the possible recoil velocities of the merger product of two spinning MBHs. For this, we use the result of Lousto et al. (2010a),

$$\vec{v} = (v_m + v_\perp \cos\xi)\hat{e}_1 + v_\perp \sin\xi \hat{e}_2 + v_\parallel \hat{e}_3. \quad (1)$$

In the last equation, the indices $\perp$ and $\parallel$ stand for perpendicular and parallel directions with respect to the orbital angular momentum vector $\vec{L}$ of the binary. $\hat{e}_1$ is a unit vector and lies on the plane of the orbit connecting the two MBHs, with direction from the heavier to the lighter one. $\hat{e}_2$ is also on the plane of the orbit, but perpendicular to $\hat{e}_1$, with direction such that $\hat{e}_1$, $\hat{e}_2$ and $\hat{e}_3$ construct a orthonormal system, with $\hat{e}_3$ defined such that is the unit vector parallel to $\vec{L}$. ξ is the angle between the unequal contributions of mass and spin to the recoil velocity. According to Gonzalez et al. (2007), $\xi \sim 145^o$ for almost circular orbits, while $\xi \sim 90^o$ in the case of head-on mergers. In the last equation,

$$v_m = A\eta^2 \frac{1-q}{1+q}(1 + B\eta), \quad (2)$$

where $v_\perp$ is the perpendicular to $\vec{L}$ component of the recoil velocity, i.e. the recoil velocity on the plane of the orbit. This is given by:

$$v_\perp = H\eta^2 \frac{1}{1+q}(a_1^\parallel - q a_2^\parallel) \quad (3)$$

and $v_\parallel$ is the parallel to $\vec{L}$ component of the recoil velocity, i.e. the recoil velocity perpendicular to the plane of the orbit,

$$v_\parallel = K\frac{\eta^2}{1+q}|a_1^\perp - q a_2^\perp| \cos(\Theta - \Theta_0). \quad (4)$$

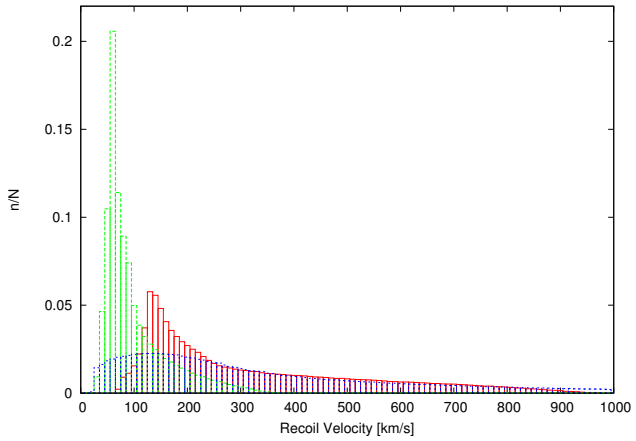

Figure 1. Histograms of the recoil velocities for different mass ratios of the binary BHs. The red, continuous line is for mass ratio $q = 0.2$, the green-dashed line for mass ratio $q = 0.1$ and the blue-dotted line for a mass ratio of $q = 1$.

In the above equations $\eta = \frac{q}{(1+q)^2}$ is the symmetric mass ratio and q is the mass ratio of the masses of the two MBHs, m_1 and m_2; $q = m_2/m_1$ with $m_2 < m_1$. According to Gonzalez et al. (2007) the values of the parameters that are involved in the above equations are: $A = 1.2 \times 10^4$ kms^{-1}, $B = -0.93$, $H = 6.9 \times 10^3$ kms^{-1}, $K = 6.072 \times 10^4$ kms^{-1}. In the last equation,

$$\vec{a}_i = \frac{\vec{S}_i}{m_i^2} \quad (5)$$

is the vector of the dimensionless spin for every one of the two BHs. Θ is the angle between vector $\vec{\Delta}$ and $\hat{e}_1$, with $\vec{\Delta}$ defined as:

$$\vec{\Delta} = (m_1 + m_2)\left(\frac{\vec{S}_2}{m_2} - \frac{\vec{S}_1}{m_1}\right) \quad (6)$$

We thus use Eq.(1) to find the most expected values for the recoil velocity of binary MBHs with different mass ratios. We deem the mass ratios of binary MBHs to be in the range $0.01 - 1$, since the observed enviromental conditions for the formation of MBHs in these CC are very similar for two random clusters **(Check this statement carefully)**. For our study, we choose three mass ratios: $q = 1$, 0.2, 0.1. For every mass ratio, we calculate the outcome of Eq.(1) using arbitrary spin magnitudes and directions and we repeate the calculations 10^7 times. We display the results for each mass ratio in Fig.(1). The histograms have a peak around the most likely velocity and a long tail to very large velocities. This is so because in order to achieve large recoil velocities, the two MBHs must be maximally spinning with the directions of their spins on the plane of the orbit and anti-parallel to each other. This is a rare case and as a result it is not very probable to have recoil velocities of the order of $\sim$ 1000km s^{-1}. We also note that the larger the mass ratio is, the shallower the distribution, so that a very broad range of velocities have almost equal probability to happen. Decreasing the mass ratio q shifts the histogram to lower velocities. The peak appears around 150km s^{-1} for

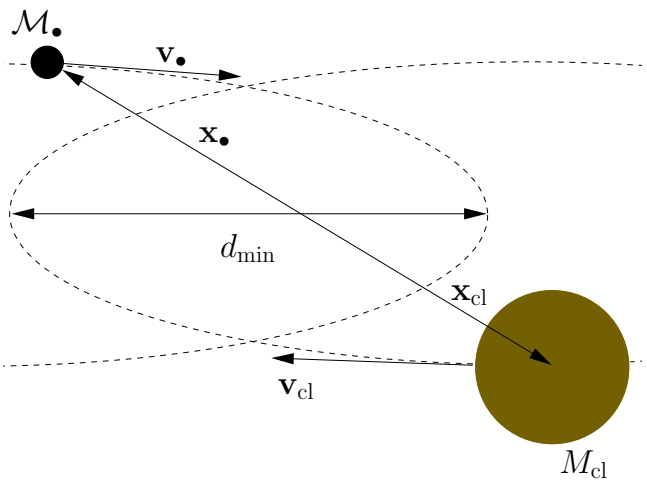

Figure 2. Geometry for the initial conditions of the parabolic collision, in the COM of the system MBH–cluster. To obtain the grid displayed in Fig.(3), we systematically vary d, $v_{\rm rel}$ and the mass ratio between the MBH and the cluster, of masses $\mathcal{M}_\bullet$ and $\mathcal{M}_{\rm cl}$

$q = 1$, $135{\rm km\,s^{-1}}$ for $q = 0.2$ and $65{\rm km\,s^{-1}}$ for $q = 0.1$. If we use lower mass ratios, the peak will move further to lower recoil velocities. For a more general study of the recoil-velocity and spin statistics see Lousto et al. (2010b). From the above we reckon that for the purposes of this study a velovity of $100{\rm km\,s^{-1}}$ is a reasonable value to assume.

3 INTERACTIONS BETWEEN A RECOILING MBH AND AN INDIVIDUAL YOUNG CLUSTER

In this section we make a study of the parameter space for a collision between a recoiling MBH and a (young individual) cluster in the CC. For this we present a set of ~ 200 direct $N-$body simulations for building a grid to cover the parameter space, which we will later feed to the simulations of the MBH in the CC.

3.1 Initial conditions for the direct $N-$body simulations for the MBH–cluster encounters

We set the MBH and the cluster on a parabolic orbit so that the minimum distance at which they pass by is $d_{\rm min}$ of Fig. (2) if they are considered to be a point particle at that moment. In the centre of mass (COM) reference frame,

$$\begin{aligned}\mathbf{x}_\bullet &= \lambda_{\rm cl}\,\mathbf{d},\\ \mathbf{x}_{\rm cl} &= -\lambda_\bullet\,\mathbf{d},\\ \mathbf{v}_\bullet &= \lambda_{\rm cl}\,v_{\rm rel},\\ \mathbf{v}_{\rm cl} &= -\lambda_\bullet\,\mathbf{v}_{\rm rel}\end{aligned} \tag{7}$$

where $\mathbf{v}_{\rm rel}$ is the relative velocity of the two objects, $\mathbf{x}_{\bullet,{\rm cl}}$ their positions (if we regard them to be a point mass, or to their centres) and $\lambda_{\bullet,{\rm cl}} = m_{\bullet,{\rm cl}}/(\mathcal{M}_\bullet + M_{\rm cl})$

We now determine $\mathbf{d}$ and $\mathbf{v}_{\rm rel}$ when the separation is d (which is given as an initial condition). Since the reduced mass is $\mu = \mathcal{M}_\bullet\,M_{\rm cl}/(\mathcal{M}_\bullet + M_{\rm cl})$, for a parabolic orbit we have that the energy at the pericentre

$$\begin{aligned}E &= \frac{-G\,\mathcal{M}_\bullet\,M_{\rm cl}}{d} + \frac{1}{2}\mu\,v_{\rm rel}^2\\ &= \frac{-G\,\mathcal{M}_\bullet\,M_{\rm cl}}{d} + \frac{1}{2}\mu\,v_{\rm max}^2 = 0.\end{aligned} \tag{8}$$

Since the specific angular momentum per unit μ is $l = l_z = -v_{\rm max}\cdot d_{\rm min} = |\mathbf{d}\wedge v_{\rm rel}|_z = x\,v_y - y\,v_x$, we obtain $v_{\rm max} = \sqrt{2\,G(\mathcal{M}_\bullet + M_{\rm cl})/d_{\rm min}}$, for a given specific angular momentum $l = \sqrt{2\,G\,d_{\rm min}(\mathcal{M}_\bullet + M_{\rm cl})}$.

As for the components of the velocities, for a given relative velocity of $v_{\rm rel} = \sqrt{2\,G\,d_{\rm min}(\mathcal{M}_\bullet + M_{\rm cl})/d}$ and with the help of the relations $-l = x\cdot v_y - y\cdot v_x$, $v_{\rm rel}^2 = v_x^2 + v_y^2$ and $d^2 = x^2 + y^2$, we can infer that the velocity components are

$$\begin{aligned}v_x &= \frac{l\cdot y}{d^2}\left[1 + \sqrt{1 + \left(\frac{d}{y}\right)^2\left(x^2\frac{v_{\rm rel}^2}{l^2} - 1\right)}\right]\\ v_y &= -\sqrt{v_{\rm rel}^2 - v_x^2}.\end{aligned} \tag{9}$$

From the definition of parabola to obtain the required expressions for x and y, $2\,d_{\rm min} - x = d$, so that $x = d - 2\,d_{\rm min}$ and $y = \sqrt{d^2 - x^2}$.

The number of stars used for the cluster is $\mathrm{N}_\star = 3\times10^3$ and we used for the initial distribution a King model of concentration $W_0 = 7$. The simulations were performed with the direct-summation $N-$body code of Aarseth Aarseth (2003). This choice was made for the sake of the accuracy of the study of the orbital parameters evolution of the binary; for this numerical tool includes both the *KS regularisation* and *chain regularisation*, which means that when two or more particles are tightly bound to each other or the separation among them becomes very small during a hyperbolic encounter, the system becomes a candidate to be regularised in order to avoid problematical small individual time steps. The basis of direct $N-$body codes relies on an improved Hermit integrator scheme (Aarseth 1999) for which we need not only the accelerations but also their time derivative. The computational effort translates into accuracy and this way we can reliably follow track of the orbital evolution of every single particle in our system.

3.2 Classification of the outcome

First we make a first guess of which particles are bound to the cluster and which ones for a bound group including the MBH (the "MBH group"). Note that a given particle can be in both group, for instance if the MBH has been captured by the cluster and has sunken to its centre or is orbiting it. For the first guess, particle are considered bound to the MBH group if they are bound to the MBH (i.e., we don't take into account the self-gravity of the bound stars themselves). For the cluster, one assumes its centre corresponds to the median position of all particles. To estimate the velocity of the cluster, one takes the average velocity of the 10% particles closest to the (assumed) centre. Particles are assumed to be member of the clusters if they are closer. The 90% particles closest to the cluster centre are assumed to be part of the cluster.

Then we iterate these attributions by computing, for

each particle, the binding energy relative to the cluster and the MBH group. For this, one has to estimate what is the position of the centre of each group and its velocity. For the MBH group, they are fixed to the values of the MBH itself. For the cluster, the centre position and velocity are defined to be the (mass-weighted) average value for all particles within hale a typical size of the previous estimate of the centre. The typical size of the cluster is the harmonic average of the distance to its centre (for all particles considered bound to it):

$$R_{\rm harm} \equiv \mathcal{M}_{\rm cl} \left(\sum \frac{m_i}{R_i} \right)^{-1} . \quad (10)$$

The gravitational energy is computed assuming a spherical mass distribution, i.e., as if each particle bound to a group (cluster or MBH group) was a spherical shell of mater, of radius R_i centred on either the MBH position or the (estimated) centre of the cluster. In general the attributions of the particles to either or both groups have converged after a few (< 10) iterations.

At the end, the attributions are "cleaned up" in the following way. If a particle belongs to both the cluster and the MBH group (and it is not the MBH), the binding energies to both structure is compared. It will be kept as member of the MBH group only if the binding energy to the MBH group is larger. In this case, it will be kept as member of the cluster (and keep its double membership) only if the MBH itself is bound to the cluster. This reduces the number of double-members in a reasonable way, still allowing for situation such as the MBH having captured some stars and being itself captured on an orbit around the (main) cluster.

Finally, to interpret the results, we allow for three kind of outcome. A "merger" is when the MBH group is bound to the cluster (as determined assuming each group is a point mass) and the distance between the centres of the groups is smaller than the sum of the $R_{\rm typ}$s. A "satellite" situation arises when the two groups are bound but the distance between their centre is larger than twice the sum of the $R_{\rm typ}$s. A "flyby" is when the groups are unbound and the distance between their centres is larger than either the sum of the total extent of each group or five times the sum of the $R_{\rm typ}$s. Any other situation would be considered as "unknown" but does not occur if the $N-$body simulation has been carried out for a sufficient amount of time.

In Fig.(4) and 5 we show two particular cases for the interaction MBH – cluster in the COM frame which, although not representative for the whole sample displayed in Fig.(3), are interesting in terms of the dynamics of the system [1] . In the first one $d_{\rm min} = 1$, which leads to an almost head-on collision between the MBH and the cluster. Still, because of the low relative velocity and mass ratio, the interaction does not lead to a huge mass loss of the cluster. Even if at $T = 45.60$ Myr the MBH and cluster seen to be unbound, the MBH is still forming a binary with the COM of the cluster and, hence, the semi-major axis decays again. After some 154 Myrs the MBH settles down to the centre and is captured. In the second figure, the larger mass ratio has a significant impact in terms of mass loss. Already after 11.62 Myr the MBH captures a portion of stars in the cluster, which remains bound to the trajectory of the hole and follow its trajectory. This satellite and the MBH are nevertheless still gravitationally bound with the cluster and fall back again on to it. The higher mass in the system MBH–satellite leads to a rather large mass loss of the original cluster. After 80.50 Myrs the MBH is at the centre of the remaining cluster.

[1] The interested reader can visit
`http://www.aei.mpg.de/~pau/dmin1_1e-2_V1kms.ogg`,
`http://www.aei.mpg.de/~pau/dmin5_3p33e-1_V3kms.ogg`
and
`http://www.aei.mpg.de/~pau/3D_dmin5_3p33e-1_V3kms.ogg`
for movies based on the results of the figures (the last URL is a 3D version of the second movie). The encoding of the movies is the free OGG Theora format and should stream automatically with a gecko-based browser (like mozilla or firefox) or with chromium or opera. Otherwise please see e.g.
`http://en.wikipedia.org/wiki/Wikipedia:Media_help_(Ogg)`
for an explanation on how to play the movies.

4 FORMING THE SEED OF AN ULTRA-COMPACT DWARF GALAXY: THE ROLE OF THE MBH

In this section we follow the evolution of the CC and the recoiling MBH. While the MBH is interacting with individual clusters, at the centre of the CC a very large cluster starts to form, which is the result of the amalgamation of smaller clusters. Of particular interest is the evolution of this very large cluster, which we will refer to as the seed UCD and the MBH. We first present in sec.(4.1) a simple estimation for the probability that the MBH hits a cluster. We will see that the timescale is well below a Hubble time, so that the study is motivated. However, in order to make a dynamical study of the system, we need to perform numerical simulations, because the architecture and distribution of clusters in the CC is also evolving in time. The central density of clusters in the CC is quickly evolving towards much higher values.

The simulations provide us with the the number of MBH–cluster hits as the MBH moves in the CC. This is important to understand whether the MBH escape or remains in the CC. In this regard, we want to find out the lowest initial escape velocity at the centre of the CC that maximises the possibility of retention of the MBH in the system and, thus, by the seed UCD. During the interactions, the MBH could trigger stellar disruptions or collisions, which could potentially be used as indicators of the capture **(In view of the two last columns of table 2 we should remove this statement probably, unless we make some kind of statistical argumentation)**.

4.1 Probability of collision MBH – cluster

For the CC we assume a Plummer sphere with a Plummer radius $\alpha = 100$pc and total radius of $R_{\rm CC} = 500$pc. The total mass in the CC is $M_{\rm CC} = 10^{8-9}{\rm M}_\odot$. We set the total number of clusters harboured in the CC to $N_{\rm cl} = 1,000$ and we set the mass of each individual cluster to $m_{\rm cl} = 10^5 M_\odot$ - $\mathcal{M}_{\rm cl} = 10^6 M_\odot$.

The escape velocity from the centre of the CC is

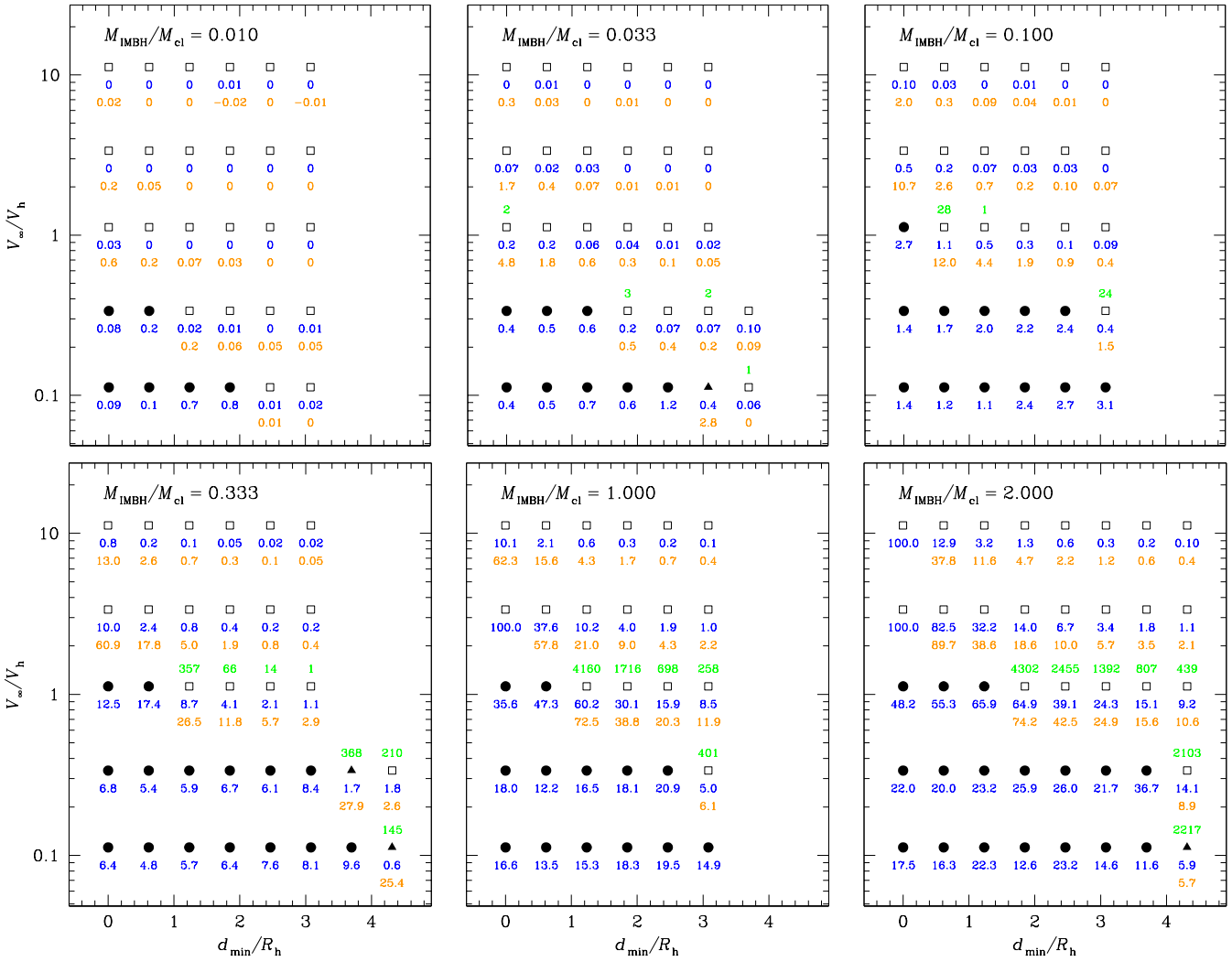

Figure 3. Outcome of all 196 simulations of encounter between a cluster with King parameter $W_0 = 7$ and an MBH. Each panel shows the results for a given mass ratio $\mathcal{M}_\bullet/\mathcal{M}_{\rm cl}$. The abscissa of each plot is the distance $d_{\rm min}$, computed assuming 2-body dynamics, in units of the half-mass radius $R_{\rm h}$. The ordinate is the relative velocity at infinity V_∞, in units of $V_{\rm h} \equiv (G\mathcal{M}_{\rm cl}/R_{\rm h})^{1/2}$, a typical velocity dispersion for the cluster. Solid round dots show "mergers", i.e., cases where the MBH has been captured by the cluster and has settled at its centre. Solid triangles are cases where the MBH is orbiting the cluster (a merger is likely to be the long-term outcome). Open squares are "fly-thrus". The number just below a symbol (in blue in the on-line colour version) is fractional mass loss from the cluster in %. The second, lower number (in orange in the on-line colour version) is the fractional reduction in specific binding energy, also in %. A number above a symbol indicates how many stellar particles are bound to the MBH (when it has not merged with the cluster).

$$v_{\rm esc}(0) = \sqrt{\frac{2G\mathcal{M}_{\rm CC}}{\alpha}} \tag{11}$$

so that for $\alpha = 100$pc, $v_{\rm esc}(0) \sim 100\ 300\,$km/s if $M_{\rm CC} = 10^{8-9}{\rm M}_\odot$.

In order to estimate the number of individual clusters in the core of the CC, we assume that the total number is $N_{\rm cl} = 1000$, that they are equal-mass, $10^6 M_\odot$. The mass of the CC at α is

$$M(\alpha) = \frac{\mathcal{M}_{\rm CC}\alpha^3}{(2\alpha^2)^{3/2}}, \tag{12}$$

with $\mathcal{M}_{\rm CC}$ the total mass of the CC. Hence, we have that $M(\alpha) = 0.354\,\mathcal{M}_{\rm CC} = 3.54{\times}10^8 M_\odot$. The number of clusters at $r = \alpha$ is:

$$N(\alpha) = \frac{M(a)}{m_{\rm cl}} \simeq 350 \tag{13}$$

The volume of the core of the CC is:

$$V(\alpha) = 4\alpha^3 \simeq 4 \times 10^6 {\rm pc}^3 \tag{14}$$

The volume of each individual cluster is:

$$\mathrm{v_{cl}} = 4\mathrm{r_{cl}^3} \tag{15}$$

Thus, if $r_{\rm cl} = 10$pc, then $\mathrm{v_{cl}} = 4 \times 10^3 {\rm pc}^3$ and the total volume of clusters in the core is $V_{\rm cl}(a) \simeq 1.4 \times 10^6 {\rm pc}^3$. If

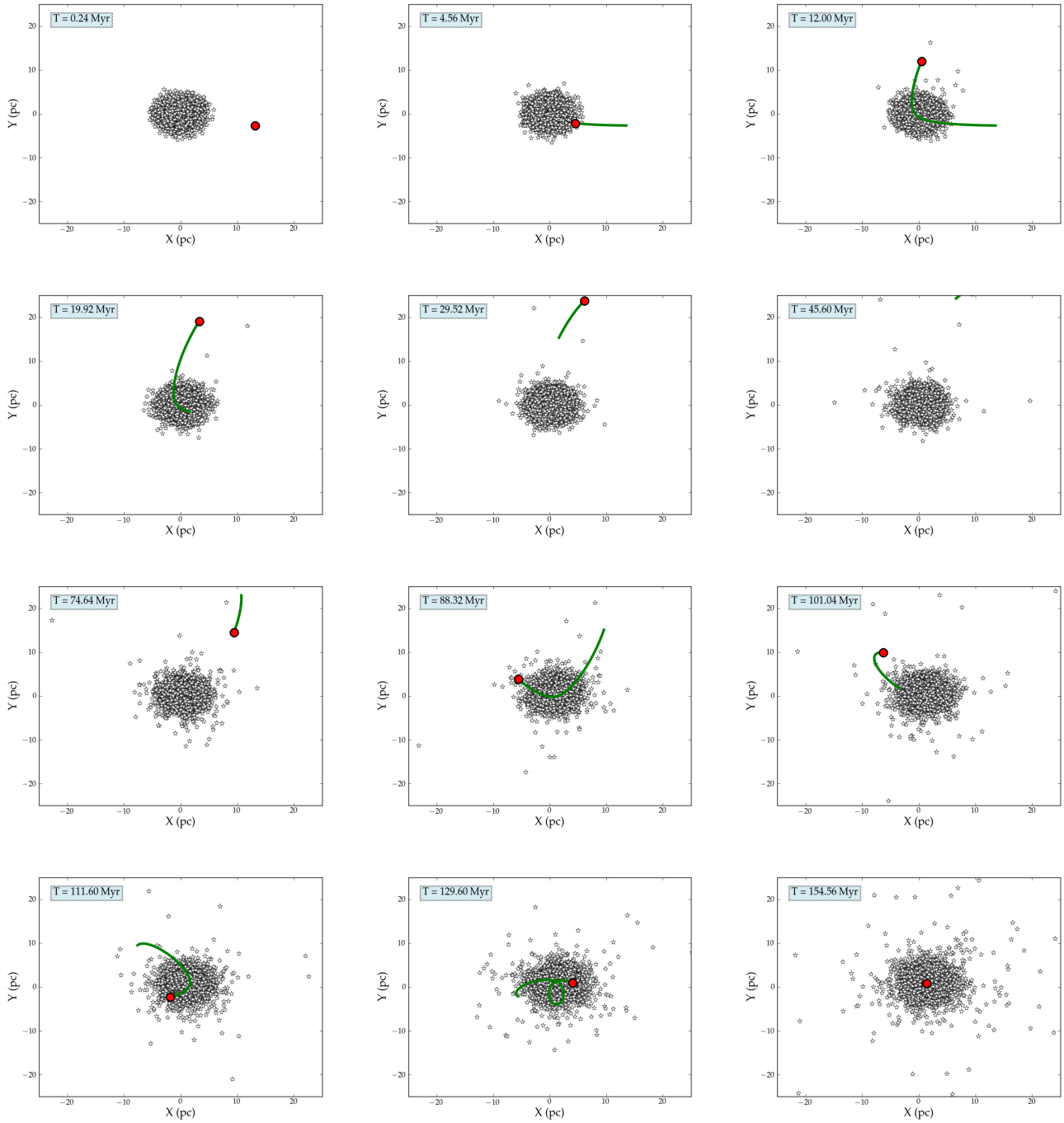

Figure 4. Projection in the X–Y plane of all trajectories of the stars (star symbols) in a cluster and the MBH (red circle) for 12 different moments in the interaction. In this particular case, the process leads to the capture of the MBH. For visibility, the radius of the MBH has been magnified by a factor 13 and the radii of the particles representing the stars by a factor 8. We additionally depict the previous 60 positions of the MBH with a solid, green line. The mass ratio between the MBH and the cluster is of 0.01, $d_{\rm min} = 1$ and $V_\infty = 1 {\rm km\,s^{-1}}$.

$r_{\rm cl} = 5{\rm pc}$, then $\mathrm{v_{cl}} = 5 \times 10^5 {\rm pc}^3$ and the total volume of clusters in the core $V_{\rm cl}(a) \simeq 1.7 \times 10^5 {\rm pc}^3$. That means that $4 - 35\%$ of the CC volume at the core is in clusters and the rest in intercluster space.

Another quantity that we need is the velocity dispersion of clusters in the CC. If the CC is in Virial equilibrium and the total kinetic energy of the cluster is $T = \frac{1}{2} M_{\rm CC} \sigma^2$ then, from the Virial theorem we have that $2T + U = 0$ and the potential energy is

$$U = -\int_0^R GM(r) dm(r) \qquad (16)$$

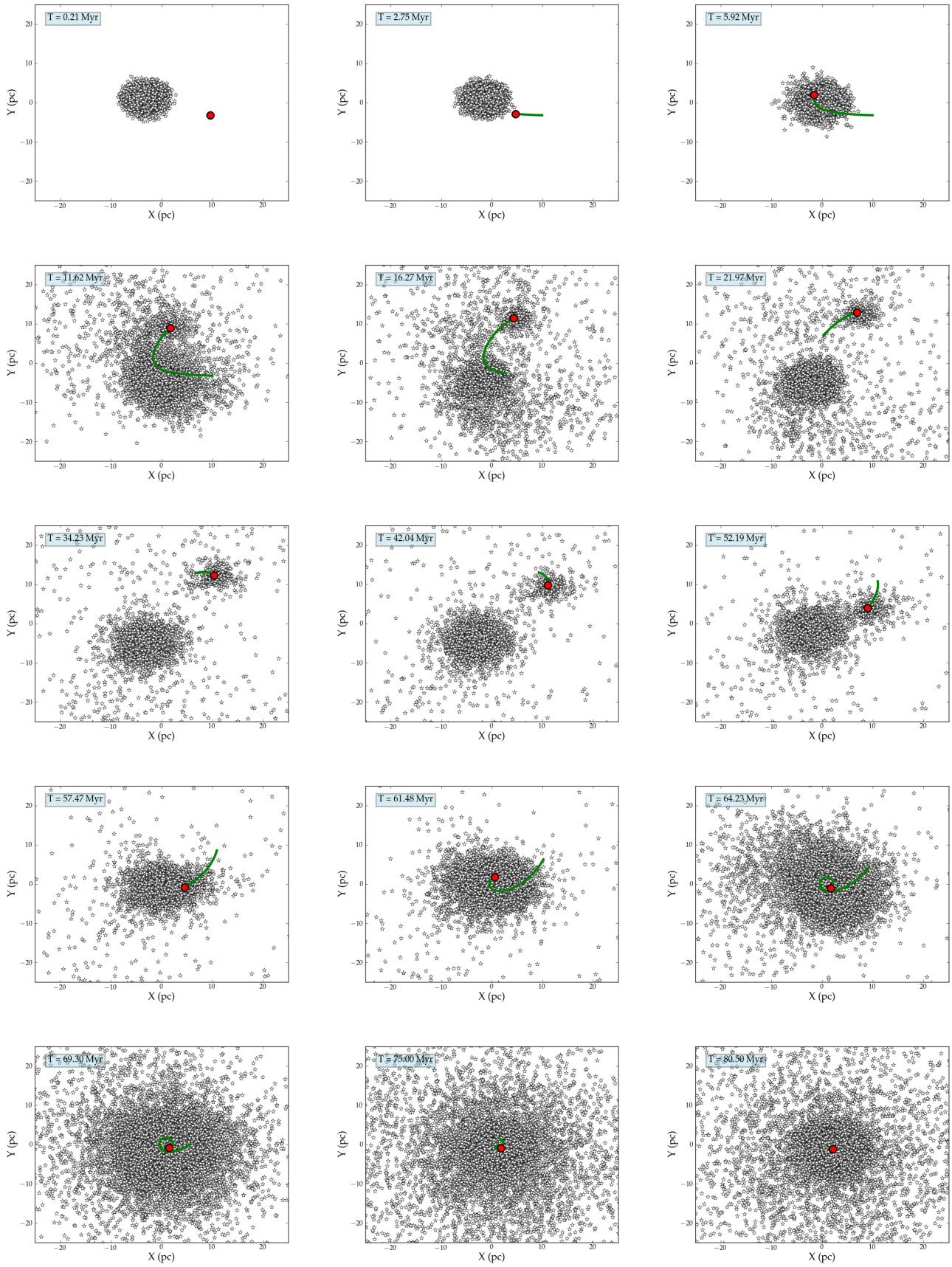

Figure 5. Same as in Fig.(4) for 15 different times. The mass ratio in this case is 0.333, $d_{\rm min} = 5$ and $V_\infty = 3 {\rm km\,s^{-1}}$.

For simplicity:

$$U = -\frac{GM_{\rm CC}^2}{R} \tag{17}$$

For $R = 500$pc the velocity dispersion is $\sigma \simeq 90$km/s. At the core radius $\sigma_{\rm core} \simeq 120$km/s. We are now in the position of calculating the cross section for an interaction MBH – cluster at the core of the CC. We assume that the individual cluster has a mass of $m_{\rm cl}$ and a $r_{\rm cl}$, the MBH has a mass $m_{\rm MBH} \ll m_{\rm cl}$ and a velocity at infinity $V_{\rm MBH}$. The impact parameter is b and the velocity of MBH at pericentre is $V_{\rm imp}$.

We can easily derive that

$$V_{\rm imp}^2 = V_{\rm MBH}^2 + \frac{2Gm_{\rm cl}}{r_{\rm cl}}, \tag{18}$$

so that, from energy and angular momentum conservation, the cross section is

$$\sigma = \pi b^2 = \pi r_{\rm cl}^2 \Big(1 + \frac{2Gm_{\rm cl}}{r_{\rm cl} V_{\rm MBH}^2}\Big) \tag{19}$$

The relative velocity $V_{\rm MBH}$ is

$$V_{\rm MBH} = V_{\rm esc} \pm V_{\rm disp}. \tag{20}$$

The positive sign is for the case that the MBH and the target cluster move in opposite directions and the negative for the case they move in the same direction. $V_{\rm disp}$ is the dispersion velocity of the clusters and $V_{\rm esc}$ is the velocity with which the MBH escapes from the host cluster (i.e. the cluster which formed after the merger of two clusters). $V_{\rm disp}$ has been approximated in the core to be $V_{\rm disp} \simeq 120{\rm km\,s^{-1}}$ and in the cluster $V_{\rm disp} \simeq 90$km/s.

From our estimate of the recoil velocity, we can assume that $V_{\rm esc}$ will be in the range $50 - 130$km/s. Actually the hole will lose a bit of kinetic energy when escaping the host cluster. Thus, the relative velocity of the MBH with respect to a cluster at the core is

$$V_{\rm MBH} = 10 - 250{\rm km/s} \tag{21}$$

And the corresponding limiting cross-sections:

$$\sigma_{10} \simeq 1428{\rm pc}^2 \tag{22}$$

and

$$\sigma_{250} \simeq 80{\rm pc}^2, \tag{23}$$

where the supscrit 10 refers to the first velocity and 250 to the second one. The average time between MBH-Cluster collisions in the core of the CC is given by:

$$\tau_{\rm MBH-cl} \sim \frac{1}{n(a)\sigma V_{\rm MBH}}, \tag{24}$$

where $n(r)$ is the number density of clusters, σ the cross-section for MBH-Cluster collision and $V_{\rm MBH}$ the relative velocity. Since we have assumed all clusters to have the same mass,

$$n(r) = \frac{M(r)}{m_{\rm cl}} = \frac{3M}{m_{\rm cl} 4\pi\alpha^3}\Big(1 + \frac{r^2}{\alpha^2}\Big)^{-5/2} \tag{25}$$

For $r = a$:

$$n(a) = \frac{3M}{m_{\rm cl} 4\pi\alpha^3} 2^{-5/2} = 4.4 \times 10^{-5} pc^{-3} \tag{26}$$

So, for the two limiting cases, $\tau_{\rm MBH-cl10} \sim 1.58$ Myr and $\tau_{\rm MBH-cl250} \sim 1.12$ Myr. In the last case, the MBH moves so fast that in the time ellapse for encounters with clusters, ~ 1Myr, it will be out of the core of the CC. The MBH loses kinetic energy as it escapes the host cluster. The difference in kinetic energy that it has at the centre and at the outskirts of the cluster is:

$$\begin{aligned} T_{\rm surf} - T_{\rm c} &= U_{\rm surf} - U_{\rm c} \\ V_{\rm es}^2 - V_{\rm rec}^2 &= 2\left(\frac{G\mathcal{M}_{\rm cl}}{(r_{\rm cl} + \alpha^2)^{1/2}} - \frac{G\mathcal{M}_{\rm cl}}{\alpha}\right) \end{aligned} \tag{27}$$

For $r_{\rm cl} = 5$pc, $\alpha = 3$pc, $\mathcal{M}_{\rm cl} = 10^6 M_\odot$ we have for a $V_{\rm rec} \sim 50 - 130{\rm km\,s^{-1}}$. I.e. the velocity of the MBH when it reaches the outskirts of the cluster is very close to the kick velocity that it received. $V_{\rm esc} \sim 44 - 127{\rm km\,s^{-1}}$.

4.2 Initial conditions for the large-scale simulations

The MBH is assumed to be the product of a merger of two MBHs that were located at the centres of two merging star clusters. Mergers of clusters happen mainly close to the centre of the CC, so it is reasonable to assume that the recoiling MBH is initially located at the centre of the CC. Also, its recoil velocity, which is of the order of $100{\rm km\,s^{-1}}$, exceeds the escape velocity of its hosting cluster, so in a small time scale the MBH is expected to escape this cluster. If the cluster has a total radius of ~ 10pc, the recoiling MBH would escape in a time-scale of ~ 0.1Myr. Hence, we decide to set up the system with the MBH initially located at the centre of the CC and not captured by any cluster.

Other than the position of the MBH there are many other parameters that can be varied in the simulations, namely the mass of the MBH, the initial velocity of the MBH which is the recoil velocity of the MBH, the mass function that the clusters follow in the CC. The observed mass function in the "knots" of the Antennæ galaxies is a power law with index $n = -2$, the upper and lower mass for the clusters, the distribution of the clusters in the CC, the total number of clusters in the CC. Observed numbers are of the order of 100, but there might be hundreds or even thousands of more low-mass clusters that are not observable (Fellhauer & Kroupa 2005). The total mass of the CC is also an additional parameter. Observations show that CCs have masses in the range $10^6 - 10^8{\rm M}_\odot$ and the total radius of the CC. The observed CCs have radii in the range $100 - 500$pc.

We choose some of the parameters according to the most expected values that are coming from observations or other studies, namely

(i) $\mathcal{M}_\bullet = 5 \times 10^3{\rm M}_\odot$.
(ii) The initial kick velocity of the MBH, $100{\rm km\,s^{-1}}$.
(iii) The mass function of the clusters is chosen to follow a power law with index $n = -2$. The masses of the clusters are discrete and come from the $\mathcal{M}_\bullet/\mathcal{M}_{\rm cl}$ ratios that were used in the MBH–cluster N-body simulations. This means that for an MBH of $\mathcal{M}_\bullet = 5 \times 10^3 M_\odot$ and $\mathcal{M}_\bullet/\mathcal{M}_{\rm cl} =$

$0.01, 0.033, 0.1, 0.33, 1, 2$, the discrete masses of the clusters in the CC are $2.5 \times 10^3 \mathrm{M}_\odot, 5 \times 10^3 \mathrm{M}_\odot, 1 \times 10^4 \mathrm{M}_\odot, 1.5 \times 10^4 \mathrm{M}_\odot, 3 \times 10^4 \mathrm{M}_\odot$ and $6 \times 10^4 \mathrm{M}_\odot$

(iv) There are no observational data about the distribution of clusters in a CC, so we assume a simple Plummer (Plummer 1911) density profile with a cut off radius

Hence, our parameter space consists of the number of clusters (N) and the initial radius ($\mathrm{R_{CC}}$) of the CC. The total mass $\mathcal{M}_{\rm CC}$ of the CC is a consequence of N, because the masses of the clusters are assumed to follow a power law. For the number of clusters, we use the values indicated in table 1. In this table, the parameters (N, $\mathcal{M}_{\rm CC}$ and $R_{\rm CC}$) of all simulations are presented, as well as an ID number.

The number of clusters might seem to high, compared with the available observations, but all the observations lack of low-mass clusters, which should also exist in CCs. Although there is no direct observation to prove that low-mass clusters also exist in CCs, there is no reason to believe that the observed power law does not continue to lower than the observed masses. Also, even if the number of clusters in our simulations is higher than expected, the total mass that we used for the CCs lies always in the limits of the observed high-mass CCs. We chose to study the high-mass CCs, because for the low-mass CCs it is almost certain that a recoiling MBH would escape the system having a very low probability of interacting with its clusters. The high-mass CCs have greater escape velocities, so the MBH would have good chances of remaining bound to the system, but even if it is escaping the CC, its velocity would decrease rapidly, which is something that favors MBH–cluster interactions. For each number N, we varied $\mathrm{R_{CC}}$ in order to create the most compact, but also the most dilute models. The total radii that we used varied from 45pc to 330pc. Given the mass and the size of the CCs, the initial escape velocities at the centres of the CCs are in the limits $27 - 137 \mathrm{km\,s^{-1}}$.

The complete set of the parameter space is shown in Figure 6, which is described below.

4.3 Evolution: Numerical experiments

The numerical code that was used for the simulations is the collisional N-body code `Myriad` (Konstantinidis & Kokkotas 2010), which uses the Hermite 4^{th} order predictor-corrector scheme with block time steps (Makino & Aarseth 1992) for advancing the particles in time, while the accelerations and their derivatives (jerks) are computed using GRAPE-6 (Makino et al. 2003) special purpose computers. Close encounters between particles are detected using the GRAPE-6 and evolved using the time-symmetric Hermite 4^{th} order integrator (Kokubo et al. 1998). Even though the code was originally designed for dynamical simulations of stars in star clusters, its modular form made its adaptation to the particular problem easy. In the simulations, every star cluster is represented by a particle. A distance, equivalent to the effective radius of the corresponding cluster, is assigned to every particle and two clusters are assumed to merge with each other when the distance between their centres becomes smaller than the sum of their radii. The search for neighboring clusters is done on the GRAPE-6. The MBH is also represented by a particle, but its radius is equal to the MBH's Schwarchild radius, i.e too small compared to the radii of the clusters.

We simulate close interactions of the MBH with a cluster using the time-symmetric Hermite $4^{\rm th}$ order integrator. During those interactions, the MBH is allowed to "pass through" the cluster, if the distance of closest approach of the two objects is smaller than the radius of the cluster. After the interaction, the MBH comes out of the cluster with a reduced kinetic energy. Using the results of detailed direct $N-$body simulations of an MBH and a star cluster presented in previous section, we find that when the interaction results a "flyby" i.e. when the MBH does not get captured by the star cluster, the kinetic energy of the MBH is reduced by a certain %. This reduction comes from the interactions of the MBH with individual stars in the cluster, which might even lead to tidal disruptions of some stars, especially in the cases of a slowly moving MBH. In the large-scale simulations of the whole CC, every-time the MBH hits a star cluster its kinetic energy is reduced according to the grid of simulations based on the individual interactions MBH–cluster. For every MBH–cluster interaction, we record:

(i) The mass ratio $\mathcal{M}_\bullet/\mathcal{M}_{\rm cl}$
(ii) The distance of closest approach $d_{\rm min}$
(iii) The relative velocity of the two objects $\mathrm{v_{inf}}$
(iv) The change in kinetic energy of the MBH

Then, from the MBH–cluster $N-$body data presented in Fig.(3), we find the outcome of the individual interaction and correct for the loss of kinetic energy of the MBH if not trapped. The individual set of MBH–cluster interactions provides us with the number of collisions of stars triggered by the presence of the MBH, the number of tidally disrupted stars by the MBH and the final outcome of the simulation. As discussed in the previous section, the final outcome might be a "flyby", a "merger" or a "satellite". In the last two cases the MBH is eventually captured by the cluster. After having the complete set of MBH–cluster interactions in a simulation, we check all of them and we record the results. We consider as the end of our simulations either the time when the MBH gets captured by a cluster, in the cases when the MBH remains bound to the CC or the time the MBH escapes the CC, in the simulations where the MBH has enough kinetic energy for this to happen.

The initial radius of each cluster depends on its mass. The most massive clusters have a half-mass radius of 4pc, while clusters with the lowest mass have half-mass radii of 0.5pc. We have applied simple laws for the result of cluster-cluster mergers. When two clusters collide we assume 20% mass-loss, so the resulting cluster has as mass the 80% of the sum of the masses and a new radius, which is equal to the radius of the most massive one plus the 20% of the sum of the radii of the two clusters. **We have to give a reason for this assumption: PAS & Freitag 2006, we reanalysed the data and this was the typical loss, or something like that**

4.4 Results

Figure 6 summarizes the results of the $N-$body simulations. Every circle represents a simulation. In the simulations in which the MBH escaped the CC after having some or no

ID	N	$M_{\rm CC}[M_\odot]$	$R_{\rm CC}$[pc]	ID	N	$M_{\rm CC}[M_\odot]$	$R_{\rm CC}$[pc]
A1	5×10^2	1.522×10^7	45	E1	3×10^3	4.32×10^7	122
A2	5×10^2	1.522×10^7	90	E2	4×10^3	5.75×10^7	165
A3	5×10^2	1.522×10^7	132	E3	4×10^3	5.75×10^7	246
A4	5×10^2	1.522×10^7	168	E4	4×10^3	5.75×10^7	329
A5	5×10^2	1.522×10^7	255				
B1	1×10^3	1.522×10^7	90	F1	5×10^3	7.18×10^7	122
B2	1×10^3	1.522×10^7	128	F2	5×10^3	7.18×10^7	165
B3	1×10^3	1.522×10^7	169	F3	5×10^3	7.18×10^7	248
B4	1×10^3	1.522×10^7	252	F4	5×10^3	7.18×10^7	330
B5	1×10^3	1.522×10^7	333				
C1	2×10^3	2.9×10^7	126	G1	6×10^3	8.6×10^7	122
C2	2×10^3	2.9×10^7	167	G2	6×10^3	8.6×10^7	165
C3	2×10^3	2.9×10^7	252	G3	6×10^3	8.6×10^7	248
C4	2×10^3	2.9×10^7	336	G4	6×10^3	8.6×10^7	330
D1	3×10^3	4.32×10^7	124	H1	8×10^3	1.14×10^8	122
D2	3×10^3	4.32×10^7	166	H2	8×10^3	1.14×10^8	165
D3	3×10^3	4.32×10^7	249	H3	8×10^3	1.14×10^8	248
D4	3×10^3	4.32×10^7	332	H4	8×10^3	1.14×10^8	330

Table 1. Number of particles, total mass and cut-off radius of the CC for the large-scale simulations.

interactions with clusters, the CC had smaller masses (simulations with IDs A1-A5, B1-B5, C1-C4, D1-D4 and E3-E4) or were less concentrated (simulations with IDs F4, G4 and H4). In the simulations where the masses and dimensions of the CC were closer to the current observational data (simulations with IDs E1-E2, F1-F3, G1-G3 and H1-H4) the IMBH remained always in the CC and gave a significant number of interactions with star clusters, until it got captured by one of them. This is so because the MBH escapes more easily from systems with a lower mass and higher radius (left-up corner of Figure 6). On the other hand, CCs with high mass and relatively small radii, have good chances of retaining the MBH (right-down corner of Figure 6).

Two examples of this are shown in Figs.(7) and (8), where we depict the formation of the seed UCD for two examples of Table 1 which led to a capture of the MBH. In these cases, the MBH has dozens of interactions with clusters with this number getting as high as ~ 100. The number of MBH–cluster interactions depends on the time it takes for the MBH to get captured by a cluster and on the density of clusters in the CC. In 6 simulations, the MBH gets captured by a cluster that has not merged with other clusters yet. In 5 simulations, the cluster that captures the MBH is the central cluster of the CC which has already increased its mass from cluster–cluster mergers. This is the UCD that starts to form from the CC. We show in table 2 the details about the cluster that captured the MBH, the position this capture took place in the CC and the mass of the most massive cluster in the system at the time of the MBH-capture. In the same table we give the number of stellar collisions that a particular simulation had **(this could be stressed much better, I guess and presented in the results)** and present an estimate of the dynamical friction time of the MBH or its hosting cluster. This time has been calculated in the following way.

The dynamical friction time ($T_{\rm DF}$) of an object with mass m moving inside a system with total mass M is given by (see e.g. Binney & Tremaine 2008)

$$T_{\rm DF} = \frac{1.17}{\ln\Lambda}\frac{\rm M}{\rm m}\frac{\rm r}{V_h}, \qquad (28)$$

where r is the distance from the centre of the system, V_h is the rms velocity dispersion of the system and $\ln\Lambda$ the Coulomb logarithm, which is of the order of unity. The dynamical friction time represents the time scale that an object of mass m needs to reach the centre of the system beginning at distance r. We employ the above formula for calculating the timescale for the MBH to reach the centre of the CC, after being captured by an individual cluster. As it is obvious from Table 2 in almost half of the simulations (5 out of 11) where the MBH was retained in the CC, the MBH gets captured by the most massive cluster of the system, the seed UCD. This cluster is the progenitor of the UCD and it is located at the centre of the CC. In those cases, the $T_{\rm DF}$ time is the required time for the MBH to reach the centre of

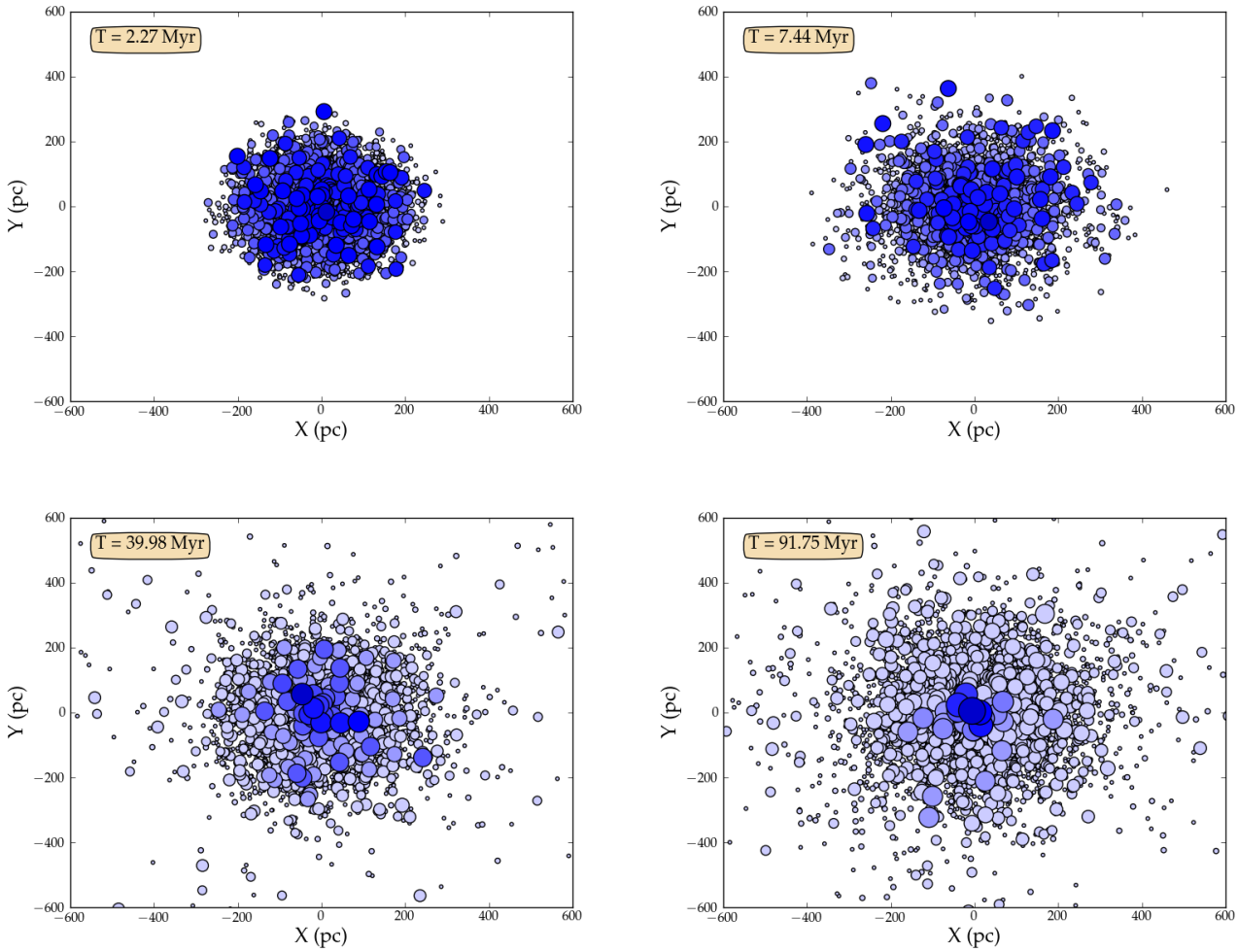

Figure 7. Formation of the UCD seed at the centre of the CC. We show a projection in the X–Y plane of all individual clusters for the simulation F3. The radii of the clusters have been artificially magnified, heavier members have larger sizes and darker colours *relative to every panel for the sake of visibility*. This means that even if the colours of the heaviest clusters in the last panel are as dark as the most massive ones in the first panel, there is no correlation, they are heavier and larger. After 7.44 Mys we can alreay see how the more massive clusters start to agglomerate at the centre of the CC. Later, at $T \sim 40$ Myr, all of them are confined to the central part of the CC and in the last panel we can see that only a handful of clusters are heavy and a very massive cluster is sitting at the very centre, while lighter clusters occupy all of the remaining space. The mass of this very massive cluster is of $2.9 \times 10^6 \mathrm{M}_\odot$ and constitutes the seed of the UCD. See `http://www.aei.mpg.de/~pau/6k_r248_rblue.ogg` for an animation of the process.

the newly formed seed UCD, so equation (28) can be written as:

$$T_{\rm DF} = \frac{1.17}{\ln\Lambda} \frac{\mathcal{M}_{\rm UCD}}{\mathcal{M}_\bullet} \frac{\rm r}{V_{\rm UCD\,,h}}. \qquad (29)$$

Where $\mathcal{M}_\bullet$ is the mass of the MBH, $\mathcal{M}_{\rm UCD}$ the mass of the seed UCD, r the radius of the UCD, which is equal to the initial distance of the MBH from its centre and $V_{\rm UCD\,,h}$ is the root mean square (RMS) dispersion velocity given by $V_{\rm UCD\,,h} = \sqrt{GM_{\rm UCD}/R_{\rm h}}$, with R_h the half-mass radius of the UCD.

On the other hand, when the MBH gets captured by a smaller cluster of the CC (6 out of the 11 simulations of Table 2), the dynamical friction time is the time required by the cluster that captured the MBH to reach the centre of the system. For this case, we can write equation (28) as follows:

$$T_{\rm DF} = \frac{1.17}{\ln\Lambda} \frac{\mathcal{M}_{\rm CC}}{\rm m_c} \frac{\rm r}{V_{\rm CC\,h}}. \qquad (30)$$

Where $\mathcal{M}_{\rm CC}$ is the mass that remained bound to the CC, $\rm m_c$ is the mass of the cluster that captured the MBH together with the mass of the MBH, r is the distance from the centre of the CC this cluster lies after capturing the MBH, and $V_{\rm CC\,h}$ is the RMS velocity dispersion of the CC. From equation (30) we can conclude that if the MBH gets captured by a cluster with a small mass, then it will take a long time to reach the centre of the CC. This is obvious in Table 2, where in the simulations where the cluster that captured the MBH was a low mass cluster, the dynamical friction time is of the order of Gyr. This estimate might be

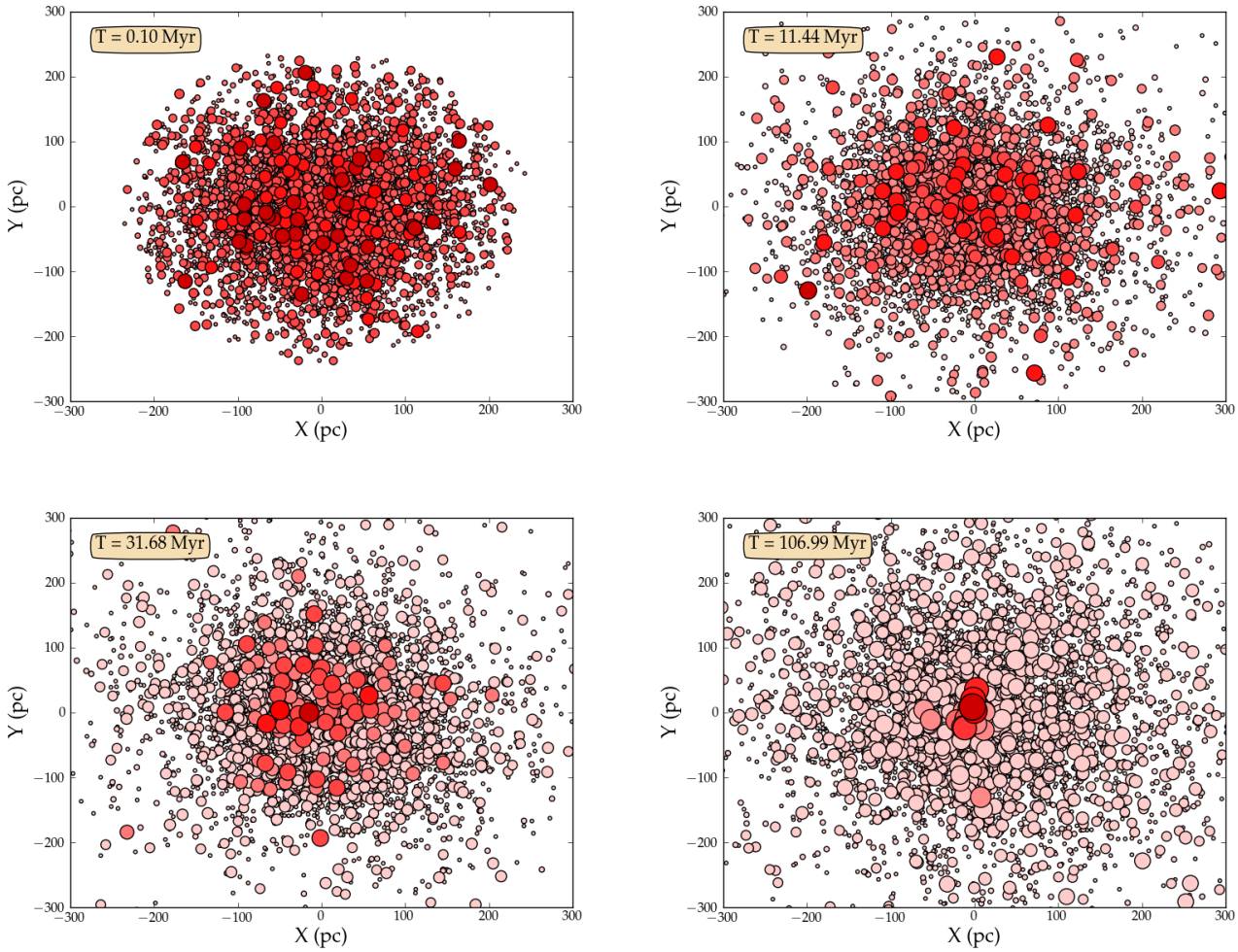

Figure 8. Same as in Fig.(7) but for simulation G3. In this case we show a zoom of diameter 600 pc. As in the first figure, after some ~ 100 Myr we have a very massive cluster at the centre and all other clusters are much lighter. The heaviest cluster at this time has a mass of $5.5 \times 10^5\,M_\odot$, while clusters with masses $5.2 \times 10^5\,M_\odot$, $5.0 \times 10^5\,M_\odot$, $1.9 \times 10^5\,M_\odot$, $1.4 \times 10^5\,M_\odot$ and $6.5 \times 10^4\,M_\odot$ lie very close to the centre of the CC. See `http://www.aei.mpg.de/~pau/5k_r248_rred.ogg` for a movie of the figure.

far from the real timescale for the MBH to reach the centre of the CC, because as the system evolves, clusters are merging with each other rapidly and the big mass concentration at the centre, will attract strongly all the remaining clusters. This is the reason that the number on the last column of Table 2 is most probably an upper limit for the real time the MBH would need to reach the centre of the CC in those cases. On the other hand, when the MBH got capture by a massive cluster, $T_{\rm DF}$ is of the order of $10 - 100$Myr. $T_{\rm DF}$ is of the order of $100 - 500$Myr in the simulations where the MBH got trapped by the UCD.

¿From the above we can make some discussion for the timescale of multiple MBH reaching the centre of a UCD formed by consecutive mergers of clusters in a CC.

The middle number next to each circle of Figure 6 is the number of stars that have been tidally disrupted from the MBH and the number of star-star collisions triggered by the MBH in the clusters. In all the simulations, there was only one tidally disrupted star (in the simulation with ID F1) so all the other numbers indicate star-star collisions triggered by the MBH. According to our results, one should expect a star-star collision in a CC every $5 - 8$Myr. In Fig.(9) we show accumulated the number of stellar collisions that led to a disruption in function of the time and the sequence of hits between the MBH and a cluster for simulation G3. We can see that there is a correlation in the number of stars torn apart and the interactions with the clusters.

The third number next to each circle of Figure 6 is the initial escape velocity at the centre of the CC. As it is obvious, CCs with initial escape velocity lower than $100{\rm km\,s^{-1}}$ may also retain an MBH with initial velocity of $100{\rm km\,s^{-1}}$. This is because of the interactions of the MBH with clusters and the energy loss of the MBH because of them. An interesting case is the simulation with ID H4 in which the escape velocity is high $84{\rm km\,s^{-1}}$, but the MBH escapes, because the system is so dilute that it has only 2 interactions with clusters. In this case, the energy of the MBH did not decrease enough to make it remain in the system. On the other hand, in the simulation G3 where the initial escape velocity at the centre of the CC is also $84{\rm km\,s^{-1}}$, the MBH

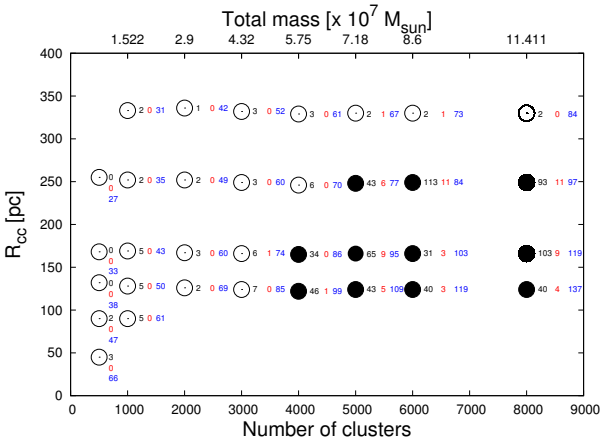

Figure 6. Outcome of the larger-scale simulations. The x-axis shows the number of clusters in each simulation, while the y-axis shows the initial radius of the CC. The upper x-axis shows the total mass of the system in $M_\odot$. Every circle corresponds to a single entry of Table 1 in a way such that the circle at the bottom left corresponds to the simulation with ID A1 and the circle at the top right corresponds to the simulation with ID H4. An open circle indicates a simulation where the MBH finally escaped the CC. On the other hand, a filled circle represents a simulation where the MBH remained bound to the system. Next to every circle there are three numbers. The first (black) shows the number of clusters hit by the MBH until either it escapes the CC or it is captured by a cluster. The second (red) number is the number of stars that are tidally disrupted by the MBH and the number of star-star collisions triggered by the MBH in the clusters. The third number indicates the initial escape velocity at the centre of the CC in $\mathrm{km\,s^{-1}}$.

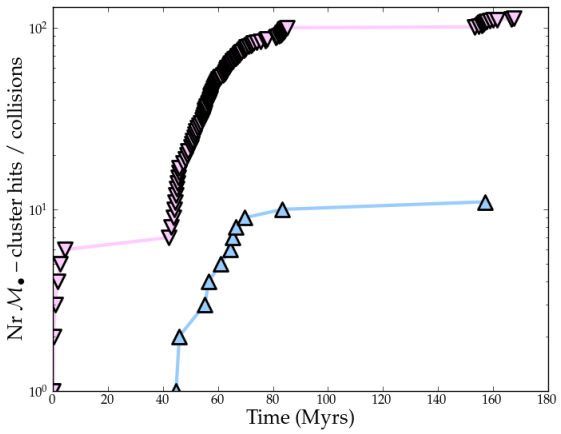

Figure 9. Cumulative number of MBH and cluster hits for the simulation G3 (inverted, light magenta triangles) and of stellar collisions leading to a disruption (blue triangles) as a function of time.

remains in the system. In this case, the system is more dense in clusters at its centre, so the MBH gives many interactions and loses enough energy that it remains bound to the CC. Figure 10 shows the evolution of the velocity of the MBH in time compared with the escape velocity at the radius of the CC where the MBH is. Initially, the escape velocity is lower

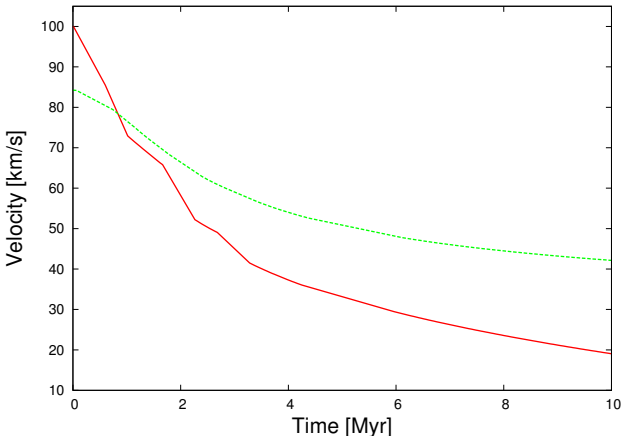

Figure 10. The velocity of the MBH as a function of time (red-continuous line) in the simulation G3, where the MBH remains in the CC. We also show the escape velocity at the point where the MBH (green-dashed line). The MBH loses energy quickly and its speed is soon lower than the escape velocity.

than the velocity of the MBH, ensuring the escape of the MBH from the system, but the MBH loses energy rapidly during the first Myr because of its interactions with clusters. After the first Myr the escape velocity at the point where the MBH exists, is continuously greater than the velocity of the MBH, so the MBH remains bound to the CC.

5 CONCLUSIONS

This has to be a bit "sexified": Any volunteers? Cole, Fred? Implications for our understanding of galaxy formation (if any), combined detection of EM and GW radiation etc etc etc

In this work we have presented results that address the formation of UCD from young clusters and the role of recoiling MBHs in a CC. For that, we have created a grid of direct-summation $N-$body simulations that covers the parameter space for MBH–cluster encounters. According to the impact parameter and relative velocity, we use the outcome from the grid to correct the loss of kinetic energy in the MBH after the interactions and to decide whether a larger-scale simulation leads to the capture of the recoiling MBH by a single cluster or not. We follow the dynamical evolution of both the recoiling MBH and the amalgamation of clusters in the CC due to dynamical friction. While the MBH interacts with individual clusters, a very large and heavy cluster starts to develop in the centre of the CC, the seed of an UCD.

In our simulations we have that the recoiling MBH almost always hits at least one cluster in the CC. The only cases where it leaves the CC without hitting a cluster are only for very dilute CCs that contain less than 1,000 clusters.

In particular, the recoiling MBH remains bound to the CC even if the initial escape velocity from the centre of the CC is lower than the initial velocity of the MBH.

In the more likely case that the MBH remains bound in the CC, it is captured by a cluster in a time scale shorter than $\sim$ 200Myr. In some of the simulations (those which had

ID	Coll	T[Myr]	R_{capt}[pc]	$\mathcal{M}_{cl}[M_\odot]$	$\mathcal{M}_{UCD}[M_\odot]$	$T_{DF}[Myr]$	T_{FH}[Myr]	T_{FC}[Myr]
E1	1	14	9.6	1.9×10^6	1.9×10^6	142	0.197	12.57
E2	0	38.2	10.3	1.2×10^6	1.2×10^6	129	0.09	33.59
F1[2]	4	9.7	42	5×10^3	6.5×10^5	2400	0.047	2.14
F2	9	28.2	18.4	7.3×10^5	7.3×10^5	240	0.067	0.54
F3	6	118	15.4	2.9×10^6	2.9×10^6	367	0.1	0.28
G1	3	10.14	45.6	2.5×10^3	1.1×10^6	4300	0.011	0.35
G2	3	13.1	23.8	1.5×10^4	6.6×10^5	762	0.009	0.009
G3	11	167.4	92.7	2.5×10^3	4×10^6	7900	0.1	44.8
H1	4	11.7	15.5	5.6×10^5	1.3×10^6	26	0.012	3.65
H2	9	20.1	17.8	1.8×10^6	1.8×10^6	360	0.15	5.32
H3	11	49.9	30.2	1.5×10^5	9.7×10^5	167	0.28	9.54

Table 2. Data for the simulations where the MBH was captured by a cluster of the CC. The first column shows the ID of the simulation (see table 1). The second column shows the number of stellar collisions triggered by the MBH. The third column displays the time of capture of the MBH by a single cluster. The fourth shows the distance from the centre of the CC, where the MBH was captured. The next column gives us the mass of that cluster and the mass of the heaviest cluster in the CC by that time; i.e. the mass of the forming UCD. The sixth column corresponds to an estimate for the MBH to reach the centre of the CC by dynamical friction (see text). The last two columns show the time the MBH hits a cluster for the first time and the time of the first stellar collision in the CC.

the largest concentrations of clusters at the centre) it gets captured by a small cluster, but in others (the ones which are less dense initially) the MBH gets captured by the seed UCD that has already formed close to the centre of the CC.

When the MBH gets captured by a small cluster, its distance from the centre of the CC is of $\sim 20-100$pc. When it gets captured by the seed UCD, its distance from the centre is approximately the radius of the seed, which is less than 20pc. In all realistic cases, the timescale for the MBH to sink down to the centre is less than 300 Myrs. In the more dilute, light clusters

In the more common case where the MBH remains bound in the CC –but also in some of the cases that it finally escapes the CC– we observe that it triggers some star-star collisional disruptions in the clusters it hits. Also, in one case, in the simulation F1 in particular, a star was tidally disrupted by the gravity of the MBH.

When the MBH remains bound to the CC, the mean time between MBH–cluster hits is $0.16-0.43$Myr. On the other hand, the mean time taken by the MBH to fly through a star cluster is of the order of 0.1Myr. Hence, after recoiling and before getting captured, the MBH spends 1/3 of its time in other clusters, while the remaining 2/3 in the inter-cluster space of the CC, so the possibility to find an MBH in a cluster of a newly formed (less than 100Myr old) CC is $\sim 30\%$

Have to make some numbers here about the estimated mass of the central massive black hole after the UCD has formed and in view of the contribution coming from potential IMBHs While the number fraction of MBH in the mass-range of $10^{2-4}\,M_\odot$ in CCs is an unknown, they sink to the centre in a time which is much shorter than the Hubble time. In that case, if we had an IMBH created every **XXX**, the UCD could be hosting a supermassive black hole of some $10^X\,M_\odot$. On the contrary to the work of Merritt et al. (2009), the internal velocities would not be as extreme as in the case of hypercompact stellar systems, since the seed UCD inherits the central velocity from the resulting mergers between individual clusters. When the UCD is formed, the velocity will roughly be what one can expect from a dense stellar system in dynamical equilibrium.

Some implications? What's special for UCD having SMBHs?

Frank et al. (2011) have resolved the inner kinematics of UCD3, the brightest known UCD in the Fornax cluster and they find that if a MBH is present, it cannot represent more than $\sim 5\%\,\mathcal{M}_{UCD}$.

ACKNOWLEDGEMENTS

It is a pleasure for PAS to thank Rainer Schödel and Emilio Alfaro for their invitation to the IAA, where the final write-up of the work was finished. He is particularly indebted with Rainer and Elena Navajas for hosting him at their place only a few weeks before their wedding, as well as for the psetta maxima. He is also thankful with Barbara Lintz and Ernst Pendl for their support during the visit to Haßloch. PAS and MCM are grateful to the Aspen Center for Physics for its hospitality during part of this project. SK is grateful to the DAAD and Luciano Rezzolla for their support during his visit at the AEI.

REFERENCES

Aarseth S. J., 1999, The Publications of the Astronomical Society of the Pacific, 111, 1333

—, 2003, Gravitational N-Body Simulations. ISBN 0521432723. Cambridge, UK: Cambridge University Press, November 2003.
Amaro-Seoane P., 2004, PhD thesis, PhD Thesis, Combined Faculties for the Natural Sciences and for Mathematics of the University of Heidelberg, Germany. VII + 159 pp. (2004), arXiv:astro-ph/0502414
Amaro-Seoane P., Freitag M., 2006, ApJ, 653, L53
Amaro-Seoane P., Santamaria L., 2009, ApJ in press
Amaro-Seoane P., Spurzem R., 2001, MNRAS, 327, 995
Amaro-Seoane P., Spurzem R., Just A., 2002, in Lighthouses of the Universe: The Most Luminous Celestial Objects and Their Use for Cosmology Proceedings of the MPA/ESO/, p. 376, p. 376
Baker J. G., Boggs W. D., Centrella J., J. K. B., T. M. S., Coleman M. M., van Meter James R., 2008, Astrophys.J., 682
Bastian N., Emsellem E., Kissler-Patig M., Maraston C., 2006, Astronomy & Astrophysics, 445, 471
Belkus H., Van Bever J., Vanbeveren D., 2007, ApJ, 659, 1576
Binney J., Tremaine S., 2008, Galactic Dynamics: Second Edition, Binney J., Tremaine S., eds. Princeton University Press
Bruens R. C., Kroupa P., Fellhauer M., Metz M., Assmann P., 2011, Astronomy & Astrophysics, accepted
Campanelli M., Lousto C., Zlochower Y., David M., 2007a, Phys.Rev.Lett., 98
Campanelli M., Lousto C. O., Zlochower Y., David M., 2007b, Astrophys.J., 659, L5
Colbert E. J. M., Miller M. C., 2005, The Tenth Marcel Grossmann Meeting. Proceedings of the MG10 Meeting held at Brazilian Center for Research in Physics, p.530
Fellhauer M., Kroupa P., 2005, MNRAS, 359, 223
Frank M. J., Hilker M., Mieske S., Baumgardt H., Grebel E. K., Infante L., 2011, MNRAS, L252+
Freitag M., Gürkan M. A., Rasio F. A., 2006a, MNRAS, 368, 141
Freitag M., Rasio F. A., Baumgardt H., 2006b, MNRAS, 368, 121
Gürkan M. A., Freitag M., Rasio F. A., 2004, ApJ, 604, 632
Gallagher S. C., Charlton J. C., Hunsberger S. D., Zaritsky D., Whitmore B. C., 2001, The Astronomical Journal, 122, 163
Gebhardt K., Rich R. M., Ho L. C., 2005, ApJ, 634, 1093
Gonzalez J. A., Hannam M., Sperhake U., Brgmann B., Husa S., 2007, Physical Review Letters, 98
Healy J., Herrmann F., Hinder I., Shoemaker D. M., Laguna P., Matzner R. A., 2009, Physical Review Letters, 102
Homeier N., Gallagher J. S. I., Pasquali A., 2002, Astronomy & Astrophysics, 391, 857
Kokubo E., Yoshinaga K., Makino J., 1998, MNRAS, 297, 1067
Konstantinidis S., Kokkotas K. D., 2010, Astronomy & Astrophysics, 522
Konstantopoulos I. S., Bastian N., Smith L. J., Westmoquette M. S., Trancho G., Gallagher J. S., 2009, The Astrophysical Journal, 701, 1015
Kroupa P., 1998, MNRAS, 300, 200
Lousto C., Campanelli M., Zlochower Y., 2010a, arXiv:0904.3541v3
Lousto C., Zlochower Y., 2008, Phys.Rev., D79
Lousto C. O., Nakano H., Zlochower Y., Campanelli M., 2010b, Phys. Rev. Letters D, 81
Lousto C. O., Zlochower Y., 2010, http://arxiv.org/abs/1011.0593
Makino J., Aarseth S. J., 1992, PASJ, 44, 141
Makino J., Fukushige T., Koga M., Namura K., 2003, PASJ, 55, 1163
Merritt D., Schnittman J. D., Komossa S., 2009, ApJ, 699, 1690
Noyola E., Gebhardt K., Kissler-Patig M., Ltzgendorf N., Jalali B., de Zeeuw P. T., Baumgardt H., 2010, The Astrophysical Journal Letters, 719, L60
Pellerin A., Meurer G. R., Bekki K., Elmegreen D. M., Wong O. I., Knezek P. M., 2010, The Astronomical Journal, 139, 1369
Plummer H. C., 1911, MNRAS, 71, 460
Portegies Zwart S. F., Baumgardt H., Hut P., Makino J., McMillan S. L. W., 2004, Nat, 428, 724
Portegies Zwart S. F., McMillan S. L. W., 2000, ApJ Lett., 528, L17
Pretorius F., 2005, Physical Review Letters, 95, 121101
Ptak A., Colbert E., 2004, The Astrophysical Journal, 606, 291
Rezzolla L., 2009, Classical and Quantum Gravity, 26, 094023
Sopuerta C. F., Yunes N., Laguna P., 2006, Physical Review D, 74, 124010
Suzuki T. K., Nakasato N., Baumgardt H., Ibukiyama A., Makino J., Ebisuzaki T., 2007, ApJ, 668, 435
Toomre A., 1977, In *The Evolution of Galaxies and Stellar Populations*, Yale, 401
van der Marel R. P., Anderson J., 2010, The Astrophysical Journal, 710, 1063
Whitmore B., 2006, "Massive Stars: From Pop III and GRBs to the Milky Way", Cambridge University Press, astro-ph/0612695
Whitmore B., Chandar R., Schweizer F., Rothberg B., Leitherer C., Rieke M., Rieke G., Blair W. P., Mengel S., Alonso-Herrero A., 2010, The Astronomical Journal, 140, 75
Whitmore B., Zhang Q., Leitherer C., Fall M., 1999, The Astronomical Journal, 118, 1551
Zhang Q., Fall S. M., 1999, The Astronomical Journal, 527, L81
Zlochower Y., Campanelli M., Lousto C. O., 2010